Since January 2020 Elsevier has created a COVID-19 resource centre with free information in English and Mandarin on the novel coronavirus COVID-19. The COVID-19 resource centre is hosted on Elsevier Connect, the company's public news and information website.

Available online at www.sciencedirect.com

SCIENCE DIRECT

Virology 332 (2005) 498–510

VIROLOGY

www.elsevier.com/locate/yviro

Programmed ribosomal frameshifting in decoding the SARS-CoV genome

Pavel V. Baranov[a,b], Clark M. Henderson[a], Christine B. Anderson[a], Raymond F. Gesteland[a], John F. Atkins[a,b], Michael T. Howard[a,*]

[a]*Department of Human Genetics, University of Utah, 15 N 2030 E, Room 7410, Salt Lake City, 84112-5330 UT, USA*
[b]*Bioscience Institute, University College Cork, Cork, Ireland*

Received 4 August 2004; returned to author for revision 7 September 2004; accepted 30 November 2004
Available online 5 January 2005

Abstract

Programmed ribosomal frameshifting is an essential mechanism used for the expression of *orf1b* in coronaviruses. Comparative analysis of the frameshift region reveals a universal shift site U_UUA_AAC, followed by a predicted downstream RNA structure in the form of either a pseudoknot or kissing stem loops. Frameshifting in SARS-CoV has been characterized in cultured mammalian cells using a dual luciferase reporter system and mass spectrometry. Mutagenic analysis of the SARS-CoV shift site and mass spectrometry of an affinity tagged frameshift product confirmed tandem tRNA slippage on the sequence U_UUA_AAC. Analysis of the downstream pseudoknot stimulator of frameshifting in SARS-CoV shows that a proposed RNA secondary structure in loop II and two unpaired nucleotides at the stem I–stem II junction in SARS-CoV are important for frameshift stimulation. These results demonstrate key sequences required for efficient frameshifting, and the utility of mass spectrometry to study ribosomal frameshifting.

Keywords: Pseudoknot; Recoding; Translation; Alternative decoding; SARS; Tandem slippage; Mass spectrometry; Frameshift; Coronavirus

Introduction

Directed switching of a proportion of translating ribosomes into a new reading frame results in the synthesis of a *trans*-frame protein product. This programmed ribosomal frameshifting is an essential mechanism governing expression of a subset of viral and cellular genes (Baranov et al., 2003; Namy et al., 2004; Stahl et al., 2002). One example is in coronaviruses, where a fixed portion of the ribosomes translating orf1a change reading frame at a specific location to decode information contained in orf1b. This translational event is essential for the synthesis of viral RNA-dependent RNA polymerase and other replication components, as *orf1b* lacks its own independent site for translation initiation. This simple mechanism for gene expression ensures that product of *orf1b* is expressed at specific levels relative to the product of *orf1a*.

Frameshifting in coronaviruses was first demonstrated in Avian Infectious Bronchitis Virus (IBV) (Brierley et al., 1989). Extensive pioneering analysis by Brierley et al. (1991, 1992), Liphardt et al. (1999), and Napthine et al. (1999) discovered that ribosomes shift translation frame at the slippery sequence U_UUA_AAC, which is invariant among known coronaviruses, and is stimulated by a downstream RNA pseudoknot structure. As predicted (Ten Dam et al., 1990), 3′ RNA pseudoknots are widely used for stimulating 1 programmed frameshifting in viruses.

Mutagenic and structural data for several of the frameshift stimulators point to key elements required for their activity [For reviews, see: (Brierley and Pennell, 2001; Giedroc et al., 2000)]. Significant differences in these key elements suggest that multiple forms of pseudoknots with differences in both secondary and ternary structures can be active frameshift stimulators. For the Mouse Mammary Tumor Virus (MMTV) pseudoknot, there is a single unpaired adenine that separates stem I from stem II. This adenine is reported to be responsible for a bend between the

* Corresponding author. Fax: +1 801 585 3910.
E-mail address: mhoward@howard.genetics.utah.edu (M.T. Howard).

0042-6822/$ - see front matter © 2004 Elsevier Inc. All rights reserved.
doi:10.1016/j.virol.2004.11.038

two stems (Shen and Tinoco, 1995) and it has been proposed that this adenine and the resulting bent conformation are essential for frameshift stimulation (Chen et al., 1995, 1996; Kang and Tinoco, 1997; Kang et al., 1996). Similarly, there is a single unpaired adenine between stems I and II in simian retrovirus type-1 (SRV-1) pseudoknot. However, unlike MMTV, altering the nucleotide in this position and the corresponding base across the stem to be either paired or unpaired does not have a dramatic effect on the efficiency of frameshifting (Sung and Kang, 1998). The crystal structure of the Beet Western Yellow Virus (BWYV) frameshift pseudoknot (Su et al., 1999) reveals several significant structural features. Notably, adenine-rich loop II forms extensive hydrogen bond interactions with stem I, and a base-triple is formed between an unpaired cytosine in loop II and stem I (Su et al., 1999). Mutagenic studies demonstrated that these interactions are critical for frameshifting efficiency (Kim et al., 1999).

A different type of pseudoknot termed "elaborated pseudoknot" or "kissing stem loops" was found to be utilized by Human Coronavirus 229E (HCV 229E) (Herold and Siddell, 1993). An alignment of frameshift cassettes from all available coronaviral sequences is shown in Fig. 1, panels A and B. RNA secondary structures proposed based on this alignment are shown in Fig. 1, panels C and D. The alignment demonstrates the potential to utilize the "elaborated pseudoknot" only in the HCV 229E, HCV NL63, PEDV, and TGV coronaviruses. In the other coronaviruses, including SARS-CoV, the proposed structure is an RNA H-type pseudoknot similar to that characterized for IBV.

The predicted pseudoknot structure of SARS-CoV, the causative agent of Severe Acute Respiratory Syndrome (Marra et al., 2003; Thiel et al., 2003), shares significant similarities to the IBV frameshift pseudoknot. However, differences occur at sites likely to be important for frameshift stimulation, such as the junction between stem I and stem II (Fig. 1C). Recently, the existence of an RNA stem loop structure within the loop II of SARS-CoV pseudoknot has been proposed (Ramos et al., 2004) suggesting that unlike IBV there may be a critical feature in loop II of the SARS-CoV pseudoknot required for frameshift stimulation.

In addition to these differences in pseudoknot sequence and possibly structure, a second putative slippery site (G_UUU_UUA) partially overlaps the predicted standard heptanucleotide shift site, U_UUA_AAC (Fig. 1A) in SARS-CoV. A similar slippery sequence (G_UUA_AAC) is used for frameshifting in Equine arteritis virus (Den Boon et al., 1991) indicating that the first position of the P-site tRNA anticodon (nucleotide 36) may not require traditional Watson Crick base pairing after shifting into the −1 reading frame.

The present study is devoted to experimental analysis of the location, mechanism and the downstream stimulator of ribosomal frameshifting in SARS-CoV.

Results

Sequence comparison of coronaviral frameshift regions

Comparisons of the frameshift regions from SARS-CoV and other coronaviruses demonstrate significant sequence homology (Figs. 1A and B). The potential for secondary structure is conserved due to compensatory variances that maintain base pairing as shown in Figs. 1A and B. In particular, the secondary structure of stem I is preserved, with its distance from the frameshift site varying between 3 and 6 nucleotides. As seen in Figs. 1A and C, stem I varies between 11 and 14 base pairs, and stem II from 5 to 9 base pairs in length. These values assume G:U and A:U pairs are formed at the ends of stems I and II although these pairings may be non-existent or only transiently formed in vivo.

In three viruses, HCV 229E, HCV NL63, and Porcine Epidemic Diarrhea Virus (PEDV), there is a bulge inside the putative stem II that makes formation of this stem highly unlikely. For HCV 229E, it has been shown that frameshifting is stimulated by a structure different from the one used in IBV (Herold and Siddell, 1993). This involves pairing of the apical loop of stem I with the apical loop of stem III located downstream to form an 'elaborated pseudoknot' or kissing stem loops (Figs. 1B, D).

All coronaviral frameshift regions contain the shifty sequence U_UUA_AAC (Fig. 1A). However, the SARS-CoV contains a second overlapping potential shift site G_UUU_UUA. Frameshifting occurs in the Equine arteritis virus at the similar frameshift site, G_UUA_AAC (Den Boon et al., 1991), where tRNALeu can pair with a GUU codon after slippage.

A distinctive feature of pseudoknots from SARS-CoV, MHV, BCV, and HCVOC43, which is not present in the well studied IBV pseudoknot, is the occurrence of two unpaired nucleotides at the stem I–stem II junction (Fig. 1A and C). In addition, a second unique feature of SARS-CoV pseudoknot is the potential for two G:U pairs at the base of the stem I (Figs. 1A and C). Comparative analysis does not provide a clear answer to whether these pairs are formed.

SARS-CoV frameshift site

SARS-CoV frameshifting levels were measured in cultured cells utilizing a dual luciferase quantitative reporter assay system. The reporter plasmid, containing the Renilla and firefly luciferase genes on either side of a multiple cloning site, can be expressed in transiently transfected tissue culture cells via the SV40 promoter (Grentzmann et al., 1998). Sequences containing wild type and mutant variants of SARS-CoV frameshift site cassettes (Fig. 2A) were cloned between the two reporter genes. Constructs were designed such that the downstream firefly luciferase gene is in the −1 reading frame and can be translated only if

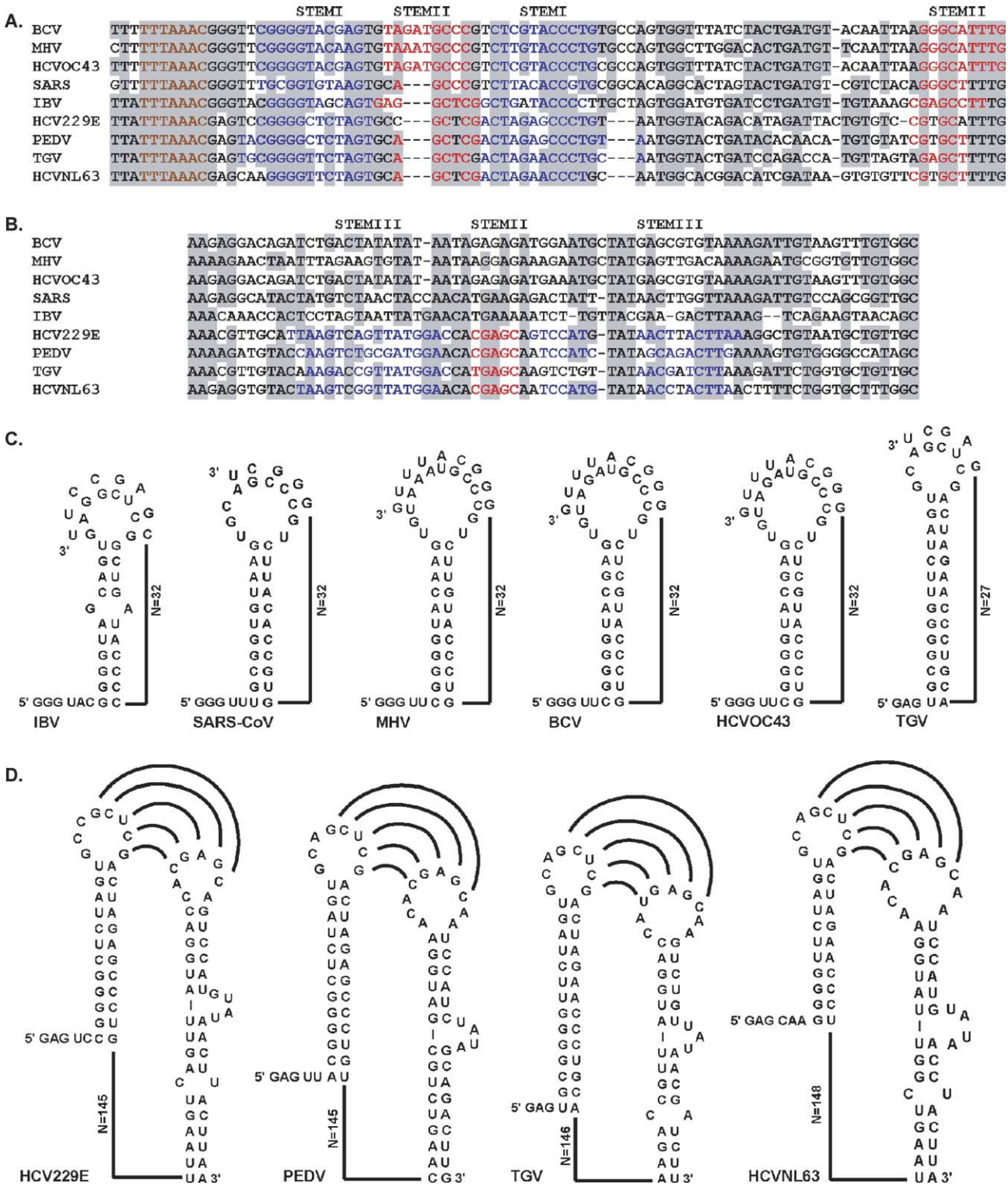

Fig. 1. Sequence comparisons and predicted structures for coronoviral frameshift sites and stimulators. A. Alignment of the regions containing frameshift site and IBV-type pseudoknot. B. Alignment of the regions containing RNA stem loop structure that participates in formation of an elaborated pseudoknot or kissing stem loops. C. Secondary structures of predicted IBV-type pseudoknots. D. Secondary structures of predicted kissing stem loops. In panels A and B shading is used to show conserved nucleotides, frameshift sites are indicated with brown color, blue is used for the stem I and also for the stem III of 'elaborated pseudoknots' and red is used for each potential stem II. The predicted structures are shown, allowing for G:U and A:U pairing to indicate the longest possible stems The length of loop II and the positions of each loop and stem are indicated. Viral names are abbreviated; Avian Infectious Bronchitis Virus (IBV); Mouse Hepatitis Virus (MHV); Bovine Coronavirus (BCV); Human coronavirus OC43, HCVOC43; Transmissible Gastroenteritis Virus (TGV); Human Coronavirus 229E (HCV229E); Porcine Epidemic Diarrhea Virus (PEDV); Human Coronavirus NL63 (HCVNL63).

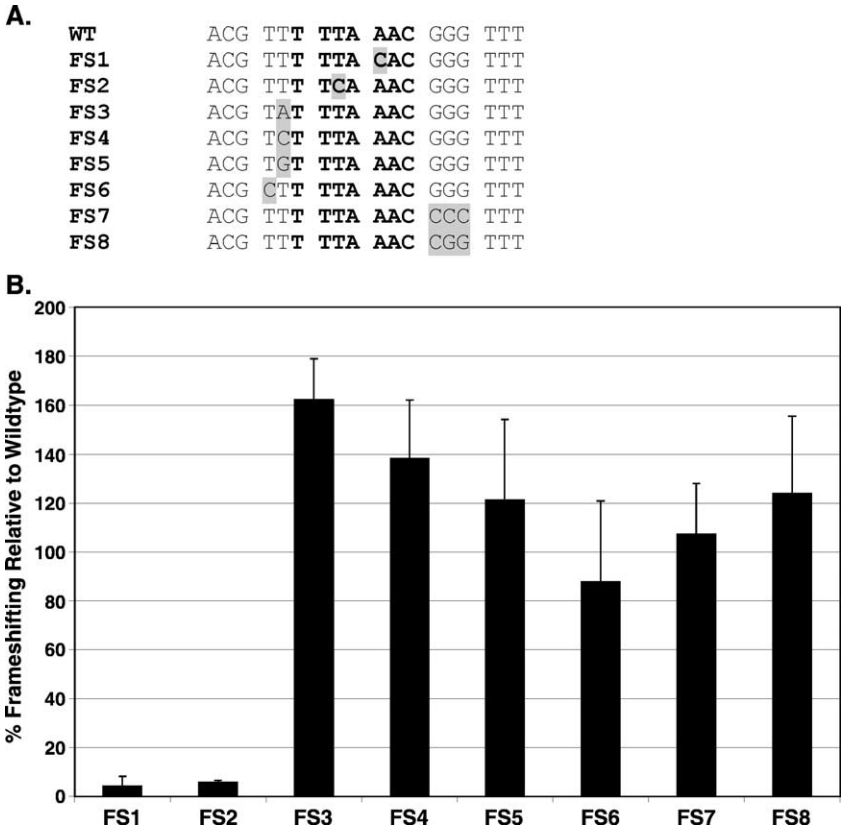

Fig. 2. Mutagenic analysis of the frameshift site. A. The sequence of the frameshift region where changes were made is shown. The entire frameshift cassette including the pseudoknot was cloned into p2luc. Frameshift site is in bold, changes are high lighted in grey. B. A histogram of the results obtained by Dual luciferase assay indicating percent frameshifting in HEK293 cells relative to wildtype frameshifting levels.

frameshifting occurs. The dual luciferase reporter constructs were then transiently transfected into cultured HEK293 cells grown in 96-well plates as described in Materials and methods. After 48 h of growth, cell lysates were prepared, and each luciferase activity was sequentially measured using an automated luminometer. Efficiency of frameshifting was calculated as the difference in firefly luciferase activities normalized to Renilla luciferase expression (See Materials and methods). Values are shown as a percentage of the SARS-CoV wildtype frameshifting levels. Frameshifting efficiencies are standardized to wildtype due to our observation that although relative changes in frameshifting levels remain consistent from experiment to experiment, the absolute frameshifting values can vary depending in part on the condition of the cultured cells (one factor is passage number). By standardizing frameshifting values to the absolute wildtype frameshifting levels observed in the same experiment, this experiment to experiment variation is corrected. Absolute values for frameshifting efficiency at the wild type SARS-CoV and IBV recoding sites across all experiments was 15 ± 3% and 12 ± 3% in HEK293 cells, respectively.

Changes of the codons corresponding to the P and A sites (U_UUA_AAC sequence to U_UCA_AAC or U_UUA_CAC) reduced frameshifting to background levels (Fig. 2A; FS1, FS2) consistent with a previous report (Thiel et al., 2003). The difference between IBV and SARS-CoV sequences 5′ of canonical shift site suggests that an alternative overlapping frameshift site may be used. In SARS-CoV, the first four nucleotides of the U_UUA_AAC heptanucleotide shift site overlaps with a putative shift site G_UUU_UUA on which tandem slippage is hypothetically possible. To check whether frameshifting occurs on this second shift site, several mutations of the U_UUA_AAC heptanucleotide sequence and 5′ flanking sequences were tested. Changes of the two nucleotides upstream of the standard heptanucleotide motif did not reduce frameshifting efficiency (Fig. 2B; FS3–FS6), demonstrating that the G_UUU_UUA sequence does not contribute significantly to frameshifting. In fact, changing the nucleotide located 5′ of the heptanucleotide shift site from a U to an A increases frameshifting efficiency by 1.6-fold relative to the wildtype levels (Fig. 2; FS3).

Bertrand et al. (2002) reported that the identity of the adjacent 3′ nucleotide can significantly impact frameshifting efficiency on the A_AAA_AAG shift site in *Escherichia coli*. In addition, nucleotides within the spacer region have potential to form base pairs with strand I of stem II or nucleotides in strand II of stem II and adjacent 3′ nucleotides. Either interaction may disrupt the predicted pseudoknot structure. Interrupting this potential interaction

by changing the three nucleotides downstream of the shift site in SARS-CoV had no significant effect on frameshifting levels (Fig. 2A; FS7 and FS8), suggesting that the identity of spacer region is not critical for frameshift stimulation.

SARS-CoV pseudoknot

Experimental data reported for the IBV pseudoknot (Brierley et al., 1989) suggests that sequences forming the pseudoknot can be varied at some positions without loss of function if the secondary structure of the pseudoknot is preserved. Mutagenic analysis of the SARS-CoV stem I and stem II was undertaken to determine critical features for ribosomal frameshifting (Fig. 3A). Disruption of stem I or II independently reduced frameshifting efficiency 10- to 20-fold (Fig. 3B; SARSPK1, 3, and 5), equivalent to levels at which ribosomal frameshifting occurs at the −1 slippery sequence in the absence of any stimulators. Restoration of the pseudoknot by "strand switching", which converts G:C, G:U, and A:U pairing to C:G, U:G, and U:A pairing, respectively (Fig. 3A; SARSPK4), of stem I restored frameshift levels to 180% of wildtype (Fig. 3B). Changing the 5′ half of stem I in SARSPK4 to the complementary sequence (Fig. 3A; SARSPK4-1) reduced frameshifting levels to 40% of wildtype (Fig. 3B) suggesting that sequence as well as the structure of this portion of stem I are important. In agreement with this observation, when stem I was restored by "stem inversion" (SARSPK2), in which the order of the base pairs in the stem are reordered from top to bottom (Fig. 3A; SARSPK2), frameshifting levels remained near background levels (Fig. 3B). A similar result was obtained by a combination of "strand switching" and "stem inversion" for SARSPK2-1 (Fig. 3). Each altered sequence was examined using mfold (Mathews et al., 1999; Zuker, 2003) for other possible folding configurations. In each case where base pairing potential was restored mfold predicted the expected pairing of strand I and II of stem I (data not shown).

Restoration of stem II (SARSPK6) by "strand switching" returned frameshifting to wildtype levels. "Stem II inversion" resulted in a reduction of frameshifting SARSPK6A (Fig. 3) to 20% of wildtype. Changing the three C:G pairs to A:U pairs (SARSPK7) further reduced frameshifting levels

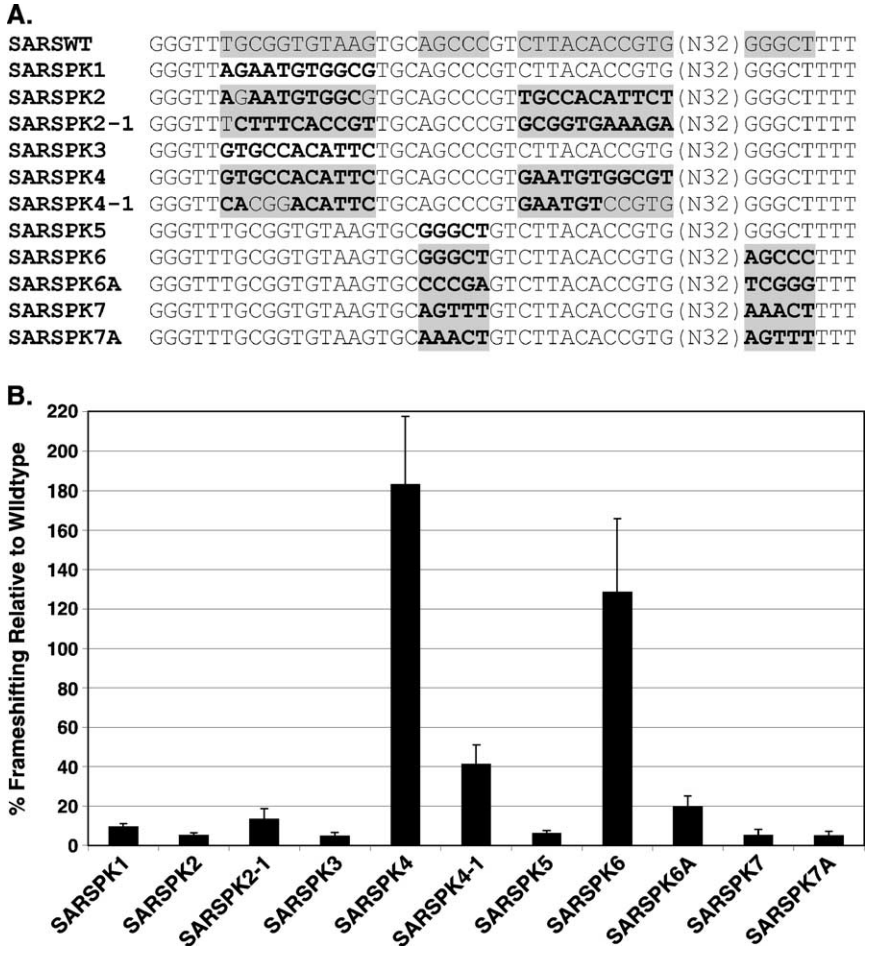

Fig. 3. Mutagenic analysis of the pseudoknot. A. The sequence of the pseudoknot region where changes were made is shown. The entire frameshift cassette was cloned into p2luc. Changed nucleotides are shown in bold. Nucleotides participating in formation of base pairs are highlighted in gray. B. A histogram of the results obtained by Dual luciferase assay indicating percent frameshifting in HEK293 cells relative to wildtype frameshifting levels.

to background and "stem switching" of SARSPK7 (SARSPK7A) did not change this level (Fig. 3B). As for stem I, it appears that both pairing potential and the sequence of stem II are important for frameshift stimulation.

According to experiments performed with the IBV pseudoknot, the sequence of loop II and its length can be varied significantly (Brierley et al., 1991) without altering frameshift efficiency. For the SARS-CoV pseudoknot, it has recently been proposed that a stem loop structure can be formed within the loop II (Ramos et al., 2004). To determine the importance of loop II in SARS-CoV, sequence portions of nine nucleotides at a time were deleted from the 3′ end of loop II and frameshift levels were measured in HEK293 cells. The first deletion had no significant effect (Fig. 4B; SARSL1). Deleting 18 nucleotides reduced frameshifting efficiency slightly to 80% (Fig. 4B; SARSL2) and further reduced to 35% of wildtype levels by deleting 27 nucleotides (Fig. 4B; SARSL3). Surprisingly, a dramatic reduction in frameshifting was observed by leaving the length unchanged but altering the sequence of loop II. Nine nucleotides at a time were changed to the complimentary sequence. Frameshifting was reduced to 35% of wildtype when 9 nucleotides located near the 3′ end of loop II were changed (Fig. 4; SARSL4). Most strikingly, changes in the middle or near the 5′ end of the loop reduced frameshifting levels to 7% and 8% of wildtype frameshifting levels, respectively (Fig. 4; SARSL5, and SARSL6). There is a potential for RNA stem loop formation in loop II (Ramos et al., 2004). Its importance for the frameshifting is not supported by the deletion mutants, in SARSL1 and

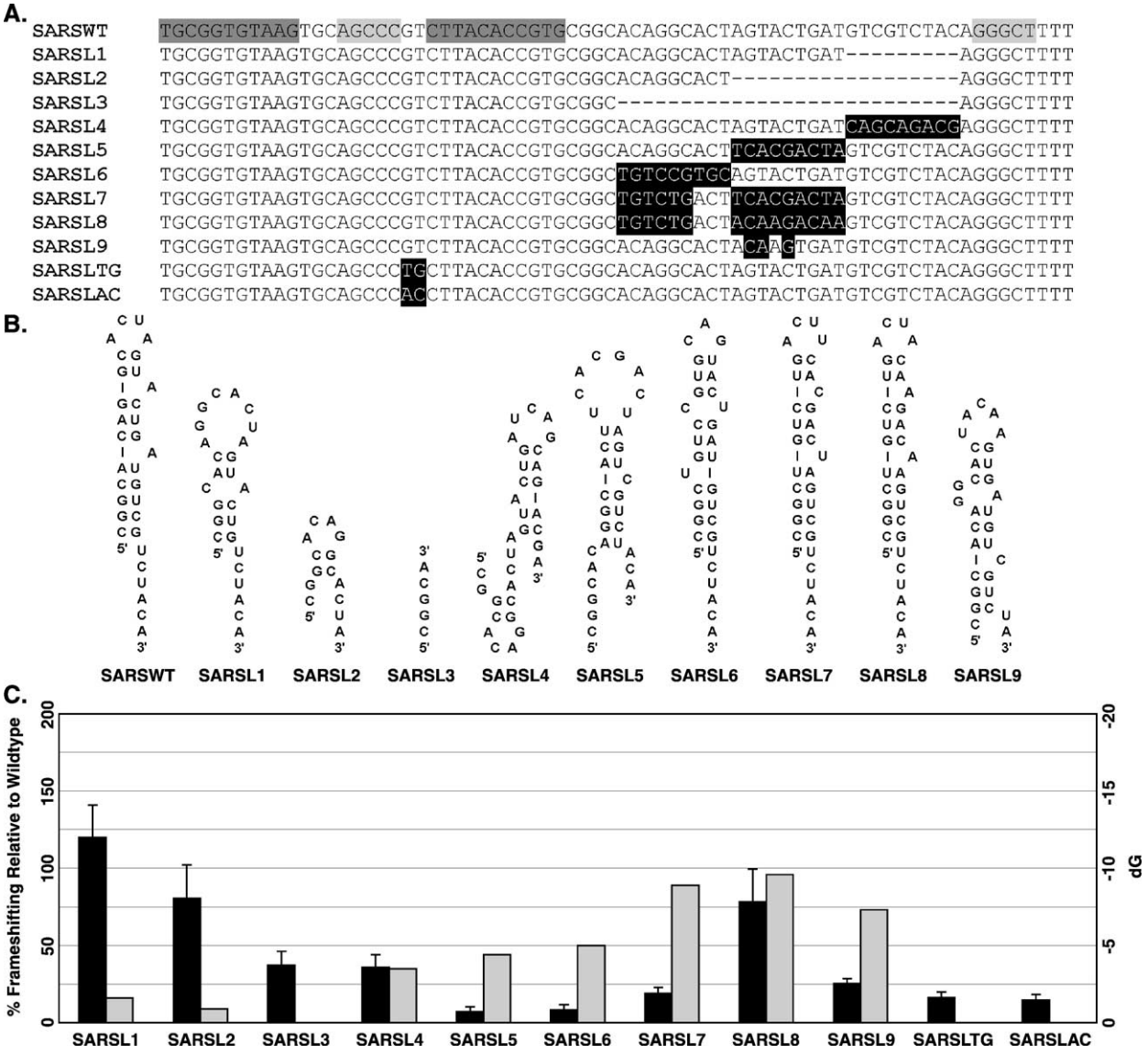

Fig. 4. Mutagenic analysis of loop II. A. The sequence of the loop II region where changes were made is shown. The entire frameshift cassette was cloned into p2luc. Changes are highlighted in black, dashes indicate deleted nucleotides. For SARSWT stem I of the pseudoknot is in gray, stem II of the pseudoknot in light gray. B. Potential RNA secondary structures in the loop II. C. A histogram of the results obtained by Dual luciferase assay indicating percent frameshifting in HEK293 cells (black bars) relative to wildtype frameshifting levels. Free energies of potential RNA secondary structures in loop II (light gray bars).

SARSL2 in which a significant part of this structure is removed (Fig. 4), but frameshifting levels remain high. However, it is possible that this stem loop is important in the context of the wildtype large loop II. To test this, we restored formation of the RNA stem loop in loop II by converting G:C and A:U pairs to C:G and U:A pairs respectively, but this change did not result in restoration of frameshifting levels (Fig. 4B; SARSL7). A notable feature of the WT stem loop is the presence of two bulged As. Unpaired or bulged adenosines are known to form A-minor motifs, a very common element of tertiary structure interactions (reviewed in Strobel 2002). In the SARSL7 construct, the bulged nucleotides in the predicted stems are changed to either C or U. By changing these nucleotides and the 3′ U in the apical loop to As (Fig. 4; SARSL8), frameshifting levels were restored to nearly wild type levels. To further confirm the importance of this stem loop, we made minimal changes (only three nucleotides were mutated) which should significantly disturb the structure of the stem loop (Fig. 4; SARSPK9). These minimal changes reduced frameshifting to background levels.

One difference noted in sequence comparisons between IBV and SARS-CoV pseudoknots was the presence of unpaired GU nucleotides near the stem junction in SARS-CoV. SARSLTG and SARSLAC were constructed to test the importance of this dinucleotide to frameshift stimulation (Fig. 4). SARSLTG extends the base pairing potential of stem I by creating complementary nucleotides between stem I and the 5′ most nucleotides of loop I. In SARSLAC, the unpaired GU nucleotides are changed to AC which maintains these nucleotides in an unpaired configuration. The predicted secondary structure of SARSLTG pseudoknot is similar to the IBV secondary structure where this extended pairing potential in stem I is observed (Fig. 1B). Both alterations reduced the ability of this pseudoknot to stimulate frameshifting to 15% of wildtype levels (Fig. 4B) demonstrating the importance of these two nucleotides for frameshift stimulation.

Mass spectrometry of the frameshift product

Frameshifting for gene expression purposes in viral genes frequently occurs on a heptanucleotide “slippery” motif, X_XXY_YYZ (Baranov et al., 2002; Hatfield et al., 1992; Jacks et al., 1988; Namy et al., 2004). A common assumption is that P- and A-site tRNAs decoding XXY and YYZ, reposition into the −1 reading frame at the overlapping XXX and YYY codons. However, this is not always the case as frameshifting in decoding an HIV frameshift cassette results in production of two protein products when it is expressed in reticulocyte lysate (Jacks et al., 1988). While 70% of the product corresponds to a product of tandem slippage of A- and P-site tRNAs, there is an additional product corresponding to frameshifting that involves either slippage of E- and P-site tRNAs (Horsfield et al., 1995) or other tRNA rearrangements inside the ribosome allowing −1 P-site tRNA slippage (Baranov et al., 2004). To examine whether a similar situation occurs during frameshifting in SARS-CoV, a molecular mass of the frameshifting product(s) was determined. The SARS-CoV frameshift region was cloned into a mammalian expression vector, flanked upstream by Glutathione-S transferase and downstream by a six histidine nickel affinity tag (see Materials and methods). This recombinant construct was expressed in cultured cells and the products of its expression analyzed by electrospray mass spectrometry. Only one significant product was detected (Fig. 5; observed MW = 45703), corresponding to the predicted mass (MW = 45703) of a protein product with leucine and asparagine being incorporated at the shift site. This result clearly indicates that frameshifting in SARS-CoV occurs only due to tandem slippage of the P-site tRNALeu and A-site tRNAAsn which takes place at the standard U_UUA_AAC slippery site.

Fig. 5. Mass spectrometry analysis of dual tagged frameshift product expressed in HEK293 cells. The mass spectrum between 40 and 50 kDa is shown. The expected mass for tandem frameshifting on U_UUA_AAC is 45702.9.

Discussion

Although 1 tandem tRNA slippage is often assumed to be the mechanism ribosome frameshifting at X_XXY_YYZ sequence motifs, −1 P-site slippage is possible at these motifs and this alternative mechanism has been shown to account for approximately 30% of frameshifting at the HIV

shift site (Jacks et al., 1988). Mutagenic analysis of the SARS-CoV heptanucleotide frameshift site presented here, suggests that frameshifting occurs at the predicted site and most probably by a tandem tRNA slippage mechanism as frameshifting levels are significantly reduced by changes in either the A- or P-site codons. To confirm the mechanism of frameshifting at this site, we report mass spectrometry of the protein product arising from frameshifting on the coronaviral frameshift site in vivo. The resulting mass indicates that frameshifting occurs after 0-frame decoding of the Asn codon and a single *trans*-frame product is produced. This result when combined with mutagenic analysis of the SARS-CoV shift site definitively identifies the mechanism of frameshifting as tandem tRNA slippage. This shows the utility of mass spectrometry analysis for determination of the location of recoding events, and for elucidation of the mechanisms involved.

Frameshifting efficiency at the wild type IBV recoding site was 12% in HEK293 cells. IBV frameshifting efficiency is lower than what has previously been reported using rabbit reticulocyte lysates (30%) (Brierley et al., 1989). However, this is not surprising since discrepancies in absolute values of frameshifting measured in different systems are not uncommon and it was observed that, in general, frameshifting efficiency is lower when measured in vivo (Grentzmann et al., 1998; Kim et al., 1999). The critical difference between in vitro and in vivo assays remains to be identified. A recent report of IBV frameshifting using the dual luciferase reporter system in cultured cells found IBV frameshifting to be even lower at approximately 4% (Ivanov et al., 2004). The lower level frameshifting reported in that study was found to be due to the exclusion of several nucleotides just downstream from the 3′ end of the IBV pseudoknot which are required for the higher level frameshifting observed in this study. Nevertheless, comparable frameshifting efficiencies were observed for the IBV and SARS-CoV reporter constructs containing the larger frameshift window used in the present study (see Materials and methods for the IBV sequence tested).

Site-directed mutagenesis of the heptanucleotide motif reduced frameshifting levels to near background. Whereas, changing the immediate surrounding sequence had no significant effect on frameshifting with the exception that altering the nucleotide preceding the heptanucleotide motif to an A produced an increase in frameshifting levels. Interestingly, in approximately half of the other coronaviruses with known genomic sequences, an A occurs in this position (See Fig. 1). A possibility for increased frameshifting in this case could be the change of encoded amino acid and consequent effect from the nascent peptide. However, other mutations leading to amino acid changes do not produce the same effect. More likely, this effect is achieved through interaction between the nucleotide preceding and the first nucleotide of the heptanucleotide motif which affects the P-site tRNA stability. Alternatively, this effect can be achieved through interactions with the E-site tRNA, as it was recently proposed as a general factor influencing −1 frameshifting in eukaryotic viruses (Bekaert and Rousset, 2005).

The importance of base pairing potential of the sequences forming stem I of the SARS-CoV pseudoknot is demonstrated by alterations which eliminate this potential or reverse the order of base pairing (Fig. 3). However, when the sequence of stem I was reversed from top to bottom but base pairing maintained, frameshifting was severely impaired. At least three factors may account for this effect. Stem I is shown on Fig. 1 with two G:U pairs at its base. It is unclear whether these base pairs are formed. If the spacer between the pseudoknot and frameshift site is the same in IBV and SARS-CoV, only one G:U pair should be formed. Reversal of stem I from top to bottom (Fig. 3, SARSPK2) potentially changes either the spacer between the frameshift site and pseudoknot or the length of stem I. Spacer length seems unlikely to be responsible for the loss of activity as small changes in spacing do not eliminate frameshifting in IBV but reduce efficiency by only several fold (Brierley et al., 1989, 1992). Another consideration is that stem I in SARS-CoV is more G:C rich at the bottom than at the top. The majority of viral pseudoknots are G:C rich at the bottom of stem I. The importance of this feature was demonstrated for IBV previously where changes of G:C pairs in the stem I to A:U pairs reduced frameshifting about 6-fold (Napthine et al., 1999). The stability of this region of frameshift stimulators is likely to be a generally important feature for inducing ribosomal frameshifting. Most −1 frameshift stimulators start 5–9 nt downstream from the end of the heptanucleotide motif. The recent crystal structure of the *T. thermophilus* ribosome with mRNA diffused into the crystal suggests that the mRNA begins to enter the ribosome 7–9 nt downstream from P-site (Yusupova et al., 2001) (placing these −1 stimulatory structures very near the entrance to the ribosome mRNA channel). During elongation, ribosomes must unwind the stem starting from this G:C rich region while the P- and A-sites are decoding the heptanucleotide motif. This observation provides a rationale for the importance of stability in this part of the pseudoknot and its distance from the shift site.

Deletions in the IBV loop (data not shown) corresponding to SARSL1 and SARSL2 did not reduce frameshifting, whereas an IBV deletion corresponding to SARSL3 decreased frameshifting by 4-fold. The large deletion in SARSL3 and the corresponding deletion in IBV reduce the loop size to 5 nt which may be too short to span the distance from stems I and II (Brierley et al., 1991). More markedly, changing the sequence of the loop II in SARS-CoV dramatically reduced frameshifting efficiency. This suggests that loop II may contribute to important structural features required for frameshift stimulation. An additional stem loop structure within loop II has been proposed recently (Ramos et al., 2004). This stem loop is not required within loop II to support high efficiency of frameshifting, since deletions in the loop II do not significantly alter frameshifting efficiency. Evolutionary importance of this stem loop is not supported

by comparative sequence analysis with other coronaviruses. However, our data suggest that in the WT context of a large loop II, it plays an important role in frameshift stimulation. Most likely, the RNA in loop II (if not properly structured) can interfere with the structure of the stimulating pseudoknot and reduce its efficiency. Our results demonstrate that the bulged As in this proposed stem loop are important for frameshifting efficiency, potentially through interactions with the rest of pseudoknot body (for example, by A-minor motif interactions (Battle and Doudna, 2002; Nissen et al., 2001). The importance of this stem loop for high efficiency frameshifting in SARS-CoV is further supported by the fact that substitutions of only three nucleotides important for the formation of this stem loop reduce frameshifting efficiency to background levels. An answer to whether loop IIs in other coronoviruses need proper folding and to what extent they can accommodate sequence changes without loss of frameshifting requires more extensive studies of pseudoknots from other coronoviruses. However, it is clear that if such requirements exist they are highly diverse among coronaviruses as evident from the lack of conservation seen in comparative sequence analysis.

Another feature found in this study is the importance of an unpaired GU tandem at the stem junction. Nucleotides at the equivalent position in IBV are base paired and disrupting the two base pairs at the top of stem I significantly reduced frameshifting efficiency, although the identity of the base pair was less important (Brierley et al., 1991). Alterations in the SARS-CoV loop I which created base pairing potential with the unpaired GU or changing the unpaired G:U to A:C significantly impaired frameshifting levels, illustrating the importance of these two unpaired nucleotides for the frameshift stimulation by this pseudoknot. These unpaired GU tandem nucleotides exist in about half of the pseudoknots shown in Fig. 1. Additional structural studies will be required to determine the role these two nucleotides play in obtaining the active pseudoknot conformation.

Despite the sequence similarity of the SARS-CoV and IBV frameshift stimulatory elements, clearly they have a number of unique distinguishing features. In addition, we have shown that, unlike IBV, RNA in loop II of the SARS-CoV pseudoknot plays an important role in frameshifting. In the context of a large loop II, this region needs to form a secondary structure with unpaired As in order to maintain frameshift stimulating activity. In SARS-CoV, the stem loop structure, and bulged As likely play a role in the proper orientation of loop II relative to other components of the RNA pseudoknot.

Materials and methods

Comparative sequence analysis of frameshifting regions

Sequences of viral genomes were extracted from Refseq database. Accession numbers are: SARS - NC_004718, IBV - NC_001451, MHV - NC_001846, HCV229E - NC_002645, TGV - NC_002306, Bovine - NC_003045, PEDV - NC_003436, HCVOC43 - NC_005147, HCVNL63 - NC_005831. For abbreviations used see legend to Fig. 1. Multiple alignments of viral sequences were generated using ClustalW (Thompson et al., 1994) and refined manually.

Luciferase reporter constructs

Complementary oligonucleotides, to make constructs containing the sequences listed below, were synthesized at the University of Utah DNA/Peptide Core Facility so that when annealed they would have appropriate ends to ligate into either the *Sal*I/*Bam*HI or the *Sal*I/*Sac*I sites of the dual luciferase vector, p2luc (Grentzmann et al., 1998). All dual luciferase constructs were verified.

SARSWT

CGCGGATGCATCAACGTTTTTAAACGGGTTTGCGGTGTAAGTGCAGCCCGTCTTACACCGTGCGGCACAGGCACTAGTACTGATGTCGTCTACAGGGCTTTTGA

IBVWT

CGGATAAGAATTATTTAAACGGGTACGGGGTAGCAGTGAGGCTCGGCTGATACCCCTTGCTAGTGGATGTGATCCTGATGTTGTAAAGCGAGCCTTTGATGTTTGTG

SARS In frame control

CGCGGATGCATCAACGTTTCGGGTTTGCGGTGTAAGTGCAGCCCGTCTTACACCGTGCGGCACAGGCACTAGTACTGATGTCGTCTACAGGGCTTTTGA

FS1

CGCGGATGCATCAACGTTTTTACACGGGTTTGCGGTGTAAGTGCAGCCCGTCTTACACCGTGCGGCACAGGCACTAGTACTGATGTCGTCTACAGGGCTTTTGA

FS2

CGCGGATGCATCAACGTTTTCAAACGGGTTTGCGGTGTAAGTGCAGCCCGTCTTACACCGTGCGGCACAGGCACTAGTACTGATGTCGTCTACAGGGCTTTTGA

FS3

CGCGGATGCATCAACGTATTTAAACGGGTTTGCGGTGTAAGTGCAGCCCGTCTTACACCGTGCGGCACAGGCACTAGTACTGATGTCGTCTACAGGGCTTTTGA

FS4

CGCGGATGCATCAACGTCTTTAAACGGGTTTGCGGTGTAAGTGCAGCCCGTCTTACACCGTGCGGCACAGGCACTAGTACTGATGTCGTCTACAGGGCTTTTGA

FS5

CGCGGATGCATCAACGTGTTTAAACGGGTTTGCGGTGTAAGTGCAGCCCGTCTTACACCGTGCGGCACAGGCACTAGTACTGATGTCGTCTACAGGGCTTTTGA

FS6
CGCGGATGCATCAACGCTTTTAAACGGG-
TTTGCGGTGTAAGTGCAGCCCGTCTTACACC-
GTGCGGCACAGGCACTAGTACTGATGTCGTCTA-
CAGGGCTTTTGA
FS7
CGCGGATGCATCAACGTTTTTAAACCC-
CTTTGCGGTGTAAGTGCAGCCCGTCTTACACC-
GTGCGGCACAGGCACTAGTACTGATGTCGTCTA-
CAGGGCTTTTGA
FS8
CGCGGATGCATCAACGTTTTTAAACCGGTT-
TGCGGTGTAAGTGCAGCCCGTCTTACACCGTG-
CGGCACAGGCACTAGTACTGATGTCGTCTACAG-
GGCTTTTGA
SARSPK1
CGCGGATGCATCAACGTTTTTAAACGGGTTAGA-
ATGTGGCGTGCAGCCCGTCTTACACCGTGCGGCAC-
AGGCACTAGTACTGATGTCGTCTACAGGGCTTTTGA
SARSPK2
CGCGGATGCATCAACGTTTTTAAACGGGTTAGA-
ATGTGGCGTGCAGCCCGTTGCCACATTCTCGGCAC-
AGGCACTAGTACTGATGTCGTCTACAGGGCTTTTGA
SARSPK2-1
CGCGGATGCATCAACGTTTTTAAACGGG-
TTTCTTTCACCGTTGCAGCCCGTGCGGTGAAA-
GACGGCACAGGCACTAGTACTGATGTCGTCTA-
CAGGGCTTTTGA
SARSPK3
CGCGGATGCATCAACGTTTTTAAACGG-
GTTGTGCCACATTCTGCAGCCCGTCTTACA-
CCGTGCGGCACAGGCACTAGTACTGATGTCGTCTA-
CAGGGCTTTTGA
SARSPK4
CGCGGATGCATCAACGTTTTTAAACGGG-
TTGTGCCACATTCTGCAGCCCGTGAATGT-
GGCGTCGGCACAGGCACTAGTACTGATGTCGTCTA-
CAGGGCTTTTGA
SARSPK4-1
CGCGGATGCATCAACGTTTTTAAACGGGTT-
CACGGACATTCTGCAGCCCGTGAATGTCCGTGCG-
GCACAGGCACTAGTACTGATGTCGTCTACAGGGC-
TTTTGA
SARSPK5
CGCGGATGCATCAACGTTTTTAAACGGG-
TTTGCGGTGTAAGTGCGGGCTGTCTTACACC-
GTGCGGCACAGGCACTAGTACTGATGTCGTCTA-
CAGGGCTTTTGA
SARSPK6
CGCGGATGCATCAACGTTTTTAAACGGG-
TTTGCGGTGTAAGTGCGGGCTGTCTTACA-
CCGTGCGGCACAGGCACTAGTACTGATGTCGTCTA-
CAAGCCCTTTGA
SARSPK6A
CGCGGATGCATCAACGTTTTTAAACGGGTTT-
GCGGTGTAAGTGCCCCGAGTCTTACACCGTGCGG-
CACAGGCACTAGTACTGATGTCGTCTACATC-
GGGTTTGA
SARSPK7
CGCGGATGCATCAACGTTTTTAAACGGG-
TTTGCGGTGTAAGTGCAGTTTGTCTTACACC-
GTGCGGCACAGGCACTAGTACTGATGTCGTCTA-
CAAAACTTTTGA
SARSPK7A
CGCGGATGCATCAACGTTTTTAAACGG-
GTTTGCGGTGTAAGTGCAAACTGTCTTACA-
CCGTGCGGCACAGGCACTAGTACTGATGTCGTCTA-
CAAGTTTTTTGA
SARSL1
CGCGGATGCATCAACGTTTTTAAACGGGTTT-
GCGGTGTAAGTGCAGCCCGTCTTACACCGTGC-
GGCACAGGCACTAGTACTGATAGGGCTTTTGA
SARSL2
CGCGGATGCATCAACGTTTTTAAACGGG-
TTTGCGGTGTAAGTGCAGCCCGTCTTACA-
CCGTGCGGCACAGGCACTAGGGCTTTTGA
SARSL3
CGCGGATGCATCAACGTTTTTAAACGGG-
TTTGCGGTGTAAGTGCAGCCCGTCTTACACC-
GTGCGGCAGGGCTTTTGA
SARSL4
CGCGGATGCATCAACGTTTTTAAACGGG-
TTTGCGGTGTAAGTGCAGCCCGTCTTACA-
CCGTGCGGCACAGGCACTAGTACTGATCAGCA-
GACGAGGGCTTTTGA
SARSL5
CGCGGATGCATCAACGTTTTTAAACGGG-
TTTGCGGTGTAAGTGCAGCCCGTCTTACA-
CCGTGCGGCACAGGCACTTCACGACTAGTCGTCTA-
CAGGGCTTTTGA
SARSL6
CGCGGATGCATCAACGTTTTTAAACGGGT-
TTGCGGTGTAAGTGCAGCCCGTCTTACACCGT-
GCGGCTGTCCGTGCAGTACTGATGTCGTCTA-
CAGGGCTTTTGA
SARSL7
CGCGGATGCATCAACGTTTTTAAACGGG-
TTTGCGGTGTAAGTGCAGCCCGTCTTACACC-
GTGCGGCTGTCTGACTTCACGACTAGTCGTCTA-
CAGGGCTTTTGA
SARSL8
CGCGGATGCATCAACGTTTTTAAACGGGTT-
TGCGGTGTAAGTGCAGCCCGTCTTACACCG-
TGCGGCTGTCTGACTACAAGACAAGTCGTCTACAG-
GGCTTTTGA
SARSL9
CGCGGATGCATCAACGTTTTTAAACGGGTTTGCG-
GTGTAAGTGCAGCCCGTCTTACACCGTGCGGCACA-
GGCACTACAAGTGATGTCGTCTACAGGGCTTTTGA
SARSLTG
CGCGGATGCATCAACGTTTTTAAACGGGTTT-
GCGGTGTAAGTGCAGCCCTGCTTACACCGTGCGG-

CACAGGCACTAGTACTGATGTCGTCTACAGGGCTTTTGA

SARSLAC

CGCGGATGCATCAACGTTTTTAAACGGGTTTGCGGTGTAAGTGCAGCCCACCTTACACCGTGCGGCACAGGCACTAGTACTGATGTCGTCTACAGGGCTTTTGA

Cell culture and transfections

The human embryonic kidney cell line, HEK 293, was obtained from ATCC and maintained as previously described (Howard et al., 2000) in the absence of antibiotics. Cells used in these studies were subcultured at 70% confluence and used between passages 7 and 15. Cells were transfected using Lipofectamine 2000 reagent (Invitrogen), using the One-day protocol in which suspension cells are added directly to the DNA complexes in 96-well plates. 25 ng DNA and 0.2 μl Lipofectamine 2000/well in 25 μl Opti-Mem (Gibco) were incubated and plated in opaque 96-well half-area plates (Costar). Cells were trypsinized, washed and added at a concentration of 4×10^4 cells/well in 50 μl DMEM, 10% FBS. Transfected cells were incubated overnight at 37° in 5% CO_2, then 75 μl DMEM, 10% FBS were added to each well, and the plates were incubated an additional 48 h.

Dual luciferase assay of ribosomal frameshifting efficiency

Luciferase activities were determined using the Dual Luciferase Reporter Assay System (Promega). Relative light units were measured on an MLX microplate luminometer (Dynex). Transfected cells were lysed in 12.5 μl lysis buffer and light emission was measured following injection of 50 μl of luminescence reagent. Frameshifting was calculated by comparing firefly/renilla luciferase ratios of experimental constructs with those of control constructs: (firefly experimental RLUs / renilla experimental RLUs) / (firefly control RLUs / renilla control RLUs) × 100. The total number of independent experiments for each construct varies between 3 and 10, in each experiment, 3 independent data points were obtained for each construct. In total between 9 and 30 data points were obtained for each construct. Frameshift values were then standardized to the wildtype frameshift levels in that experiment, and for each construct they are as a percentage of the wildtype ((firefly experimental RLUs / renilla experimental RLUs) / (firefly control RLUs / renilla control RLUs) × 100) / percent wildtype frameshifting. For each construct all data points were then averaged and the standard deviation calculated. Data points which fell greater than 2 standard deviations from the mean were discarded as outliers.

Protein expression and purification for mass spectrometry

A mammalian expression vector producing a triple tagged (GST, Maltose Binding Protein (MBP), and 6 Histidine) tagged fusion protein was constructed as follows: pCMV Sport-Bgal (Invitrogen) was digested with *Pst*1 and *Hin*dIII and purified by agarose gel electrophoresis to remove the B-gal gene. A DNA fragment containing *Pst*1 and *Hin*dIII restriction sites, GST, MBP and 6 Histidine tags was produced by PCR amplification from plasmid GST-MBP-6xHis described in (Herr et al., 2001) using the primers; GAAGGCCTGCAGGTCACCATGTCGTTTTCCCCTATACTAGGTTATTGG, and GCGACGGCAAGCTTTATTAATGATGATGATGATGATGGTG. This fragment was cloned into the *Pst*I and *Hin*dIII sites of pCMV Sport Bgal to produce, pSport GMH. The SARS frameshift cassette was inserted into the *Bam*HI and *Eco*RI sites located between the GST and MBP genes by annealing synthetic oligonucleotides such that the sequence located between the restriction sites is derived entirely from SARS-CoV; CGTTTTTAAACGGGTTTGCGGTGTAAGTGCAGCCCGTCTTACACCGTGCGGCACAGGCACTAGTACTGATGTCGTCTACAGGGCTTTTGATAT. The resulting plasmid pSport GMH SARS1 was utilized in the Freestyle 293 expression system (Invitrogen). 90 ml of HEK293 F suspension cells were transfected with pSport GMH SARS1 using 293fectin (Invitrogen) as described by the manufacturer. After 48 h of incubation, the cells were lysed in PBS + 0.5% trition X-100 + protease inhibitors by 3× Dounce homogenization. The GST-SARS-MBP-6XHis fusion protein was purified by sequential passage over Glutathione sepharose 4B (Amersham) and Ni-NTA Agarose (Qiagen). The final product was concentrated and washed with ultrapure water 3× using a centrifugal filter device, Ultrafree-15 (Millipore). The final product was digested with PreScission protease (AP biotech) as recommended.

Protein sample Prep and ESI/MS analysis

Final desalting for mass spectrometry was performed using a C18 P10 Ziptip (Millipore). Prior to loading the protein sample onto the Ziptip, the Ziptip was washed with 50 μl of acetonitrile containing 1% formic acid, then equilibrated with 20 μl of 15% acetonitrile (and 0.5% TFA). Methanol and TFA were added to the protein sample to a final concentration of 5% and 0.5%, respectively. The protein sample was then loaded onto the Ziptip by pipetting up and down several times. To desalt the protein, the Ziptip was washed with 40 μl of 15% acetonitrile (and 0.5% TFA) then washed with 40 μl of nano-pure water. The protein was eluted from the Ziptip with 2 aliquots of 1 μl of 55% acetonitrile (and 1% formic acid) followed by 2 aliquots of 1 μl of 80% acetonitrile (and 1% formic acid). The aliquots were combined for mass spectrometry analysis.

The protein was introduced into the mass spectrometer by infusion at 3 μl/min. Mass measurements were performed with a Quattro II mass spectrometer (Micromass, Inc.) using positive-ion electrospray ionization. The

instrument was scanned from 800 to 1400 kDa in 4 s at unit resolution with 3 kV spray voltage and 55 eV cone voltage and scans were accumulated for 1 to 2 min. All spectra were acquired using Masslynx software (Micromass) and multiply-charged ion series were processed into molecular-mass spectra using MaxEnt software (Micromass, Inc.).

Acknowledgments

We thank Chad Nelson for assistance with mass spectrometry. This work was supported by NIH grant GM48152 and a grant from Science Foundation Ireland to J.F.A. and DOE grant DE-FG03-O1ER63132 to R.F.G.

References

Baranov, P.V., Gesteland, R.F., Atkins, J.F., 2002. Recoding: translational bifurcations in gene expression. Gene 286 (2), 187–201.

Baranov, P.V., Gurvich, O.L., Hammer, A.W., Gesteland, R.F., Atkins, J.F., 2003. Recode 2003. Nucleic Acids Res. 31 (1), 87–89.

Baranov, P.V., Gesteland, R.G., Atkins, J.F., 2004. P-site tRNA is a crucial initiator of ribosomal frameshifting. RNA 10 (2), 221–230.

Battle, D.J., Doudna, J.A., 2002. Specificity of RNA-RNA helix recognition. Proc. Natl. Acad. Sci. U. S. A. 99 (18), 11676–11681.

Bekaert, M, Rousset, J.P., 2005. An extended signal involved in eukaryotic −1 frameshifting operates through modification of the E-site tRNA. Mol. Cell (in press).

Bertrand, C., Prere, M.F., Gesteland, R.F., Atkins, J.F., Fayet, O., 2002. Influence of the stacking potential of the base 3′of tandem shift codons on −1 ribosomal frameshifting used for gene expression. RNA 8 (1), 16–28.

Brierley, I., Pennell, S., 2001. Structure and function of the stimulatory RNAs involved in programmed eukaryotic 1 ribosomal frameshifting. Cold Spring Harbor Symposia on Quantitative Biology. Cold Spring Harbor Laboratory Press, pp. 233–248.

Brierley, I., Digard, P., Inglis, S.C., 1989. Characterization of an efficient coronavirus ribosomal frameshifting signal: requirement for an RNA pseudoknot. Cell 57 (4), 537–547.

Brierley, I., Rolley, N.J., Jenner, A.J., Inglis, S.C., 1991. Mutational analysis of the RNA pseudoknot component of a coronavirus ribosomal frameshifting signal. J. Mol. Biol. 220 (4), 889–902.

Brierley, I., Jenner, A.J., Inglis, S.C., 1992. Mutational analysis of the "slippery-sequence" component of a coronavirus ribosomal frameshifting signal. J. Mol. Biol. 227 (2), 463–479.

Chen, X., Chamorro, M., Lee, S.I., Shen, L.X., Hines, J.V., Tinoco Jr., I., Varmus, H.E., 1995. Structural and functional studies of retroviral RNA pseudoknots involved in ribosomal frameshifting: nucleotides at the junction of the two stems are important for efficient ribosomal frameshifting. EMBO J. 14 (4), 842–852.

Chen, X., Kang, H., Shen, L.X., Chamorro, M., Varmus, H.E., Tinoco Jr., I., 1996. A characteristic bent conformation of RNA pseudoknots promotes −1 frameshifting during translation of retroviral RNA. J. Mol. Biol. 260 (4), 479–483.

den Boon, J.A., Snijder, E.J., Chirnside, E.D., de Vries, A.A., Horzinek, M.C., Spaan, W.J., 1991. Equine arteritis virus is not a togavirus but belongs to the coronaviruslike superfamily. J. Virol. 65 (6), 2910–2920.

Giedroc, D.P., Theimer, C.A., Nixon, P.L., 2000. Structure, stability and function of RNA pseudoknots involved in stimulating ribosomal frameshifting. J. Mol. Biol. 298 (2), 167–185.

Grentzmann, G., Ingram, J.A., Kelly, P.J., Gesteland, R.F., Atkins, J.F., 1998. A dual-luciferase reporter system for studying recoding signals. RNA 4 (4), 479–486.

Hatfield, D.L., Levin, J.G., Rein, A., Oroszlan, S., 1992. Translational suppression in retroviral gene expression. Adv. Virus Res. 41, 193–239.

Herold, J., Siddell, S.G., 1993. An 'elaborated' pseudoknot is required for high frequency frameshifting during translation of HCV 229E polymerase mRNA. Nucleic Acids Res. 21, 5838–5842.

Herr, A.J., Nelson, C.C., Wills, N.M., Gesteland, R.F., Atkins, J.F., 2001. Analysis of the roles of tRNA structure, ribosomal protein L9, and the bacteriophage T4 gene 60 bypassing signals during ribosome slippage on mRNA. J. Mol. Biol. 309 (5), 1029–1048.

Horsfield, J.A., Wilson, D.N., Mannering, S.A., Adamski, F.M., Tate, W.P., 1995. Prokaryotic ribosomes recode the HIV-1 *gag-pol* −1 frameshift sequence by an E/P site post-translocation simultaneous slippage mechanism. Nucleic Acids Res. 23 (9), 1487–1494.

Howard, M.T., Shirts, B.H., Petros, L.M., Flanigan, K.M., Gesteland, R.F., Atkins, J.F., 2000. Sequence specificity of aminoglycoside-induced stop codon readthrough: potential implications for treatment of Duchenne muscular dystrophy. Ann. Neurol. 48 (2), 164–169.

Ivanov, I.P., Anderson, C.B., Gesteland, R.F., Atkins, J.F., 2004. Identification of a new antizyme mRNA +1 frameshifting stimulatory pseudoknot in a subset of diverse invertebrates and its apparent absence in intermediate species. J. Mol. Biol. 339 (3), 495–504.

Jacks, T., Power, M.D., Masiarz, F.R., Luciw, P.A., Barr, P.J., Varmus, H.E., 1988. Characterization of ribosomal frameshifting in HIV-1 *gag-pol* expression. Nature 331 (6153), 280–283.

Kang, H., Tinoco Jr., I., 1997. A mutant RNA pseudoknot that promotes ribosomal frameshifting in mouse mammary tumor virus. Nucleic Acids Res. 25 (10), 1943–1949.

Kang, H., Hines, J.V., Tinoco Jr., I., 1996. Conformation of a non-frameshifting RNA pseudoknot from mouse mammary tumor virus. J. Mol. Biol. 259 (1), 135–147.

Kim, Y.G., Su, L., Maas, S., O'Neill, A., Rich, A., 1999. Specific mutations in a viral RNA pseudoknot drastically change ribosomal frameshifting efficiency. Proc. Natl. Acad. Sci. U. S. A. 96 (25), 14234–14239.

Liphardt, J., Napthine, S., Kontos, H., Brierley, I., 1999. Evidence for an RNA pseudoknot loop–helix interaction essential for efficient-1 ribosomal frameshifting. J. Mol. Biol. 288 (3), 321–335.

Mathews, D.H., Sabina, J., Zuker, M., Turner, D.H., 1999. Expanded sequence dependence of thermodynamic parameters improves prediction of RNA secondary structure. J. Mol. Biol. 288 (5), 911–940.

Marra, M.A., Jones, S.J., Astell, C.R., Holt, R.A., Brooks-Wilson, A., Butterfield, Y.S., Khattra, J., Asano, J.K., Barber, S.A., Chan, S.Y., Cloutier, A., Coughlin, S.M., Freeman, D., Girn, N., Griffith, O.L., Leach, S.R., Mayo, M., McDonald, H., Montgomery, S.B., Pandoh, P.K., Petrescu, A.S., Robertson, A.G., Schein, J.E., Siddiqui, A., Smailus, D.E., Stott, J.M., Yang, G.S., Plummer, F., Andonov, A., Artsob, H., Bastien, N., Bernard, K., Booth, T.F., Bowness, D., Czub, M., Drebot, M., Fernando, L., Flick, R., Garbutt, M., Gray, M., Grolla, A., Jones, S., Feldmann, H., Meyers, A., Kabani, A., Li, Y., Normand, S., Stroher, U., Tipples, G.A., Tyler, S., Vogrig, R., Ward, D., Watson, B., Brunham, R.C., Krajden, M., Petric, M., Skowronski, D.M., Upton, C., Roper, R.L., 2003. The Genome sequence of the SARS-associated coronavirus. Science 300 (5624), 1399–1404.

Namy, O., Rousset, J.P., Napthine, S., Brierley, I., 2004. Reprogrammed genetic decoding in cellular gene expression. Mol. Cell 13 (2), 157–168.

Napthine, S., Liphardt, J., Bloys, A., Routledge, S., Brierley, I., 1999. The role of RNA pseudoknot stem 1 length in the promotion of efficient-1 ribosomal frameshifting. J. Mol. Biol. 288 (3), 305–320.

Nissen, P., Ippolito, J.A., Ban, N., Moore, P.B., Steitz, T.A., 2001. RNA tertiary interactions in the large ribosomal subunit: the A-minor motif. Proc. Natl. Acad. Sci. U. S. A. 98 (9), 4899–4903.

Ramos, F.D., Carrasco, M., Doyle, T., Brierley, I., 2004. Programmed −1 ribosomal frameshifting in the SARS coronavirus. Biochem. Soc. Trans. 32 (Pt. 6), 1081–1083.

Shen, L.X., Tinoco Jr., I., 1995. The structure of an RNA pseudoknot that causes efficient frameshifting in mouse mammary tumor virus. J. Mol. Biol. 247 (5), 963–978.

Stahl, G., McCarty, G.P., Farabaugh, P.J., 2002. Ribosome structure: revisiting the connection between translational accuracy and unconventional decoding. Trends Biochem. Sci. 27 (4), 178–183.

Strobel, S.A., 2002. Biochemical identification of A-minor motifs within RNA tertiary structure by interference analysis. Biochem. Soc. Trans. 30 (Pt. 6), 1126–1131.

Su, L., Chen, L., Egli, M., Berger, J.M., Rich, A., 1999. Minor groove RNA triplex in the crystal structure of a ribosomal frameshifting viral pseudoknot. Nat. Struct. Biol. 6 (3), 285–292.

Sung, D., Kang, H., 1998. Mutational analysis of the RNA pseudoknot involved in efficient ribosomal frameshifting in simian retrovirus−1. Nucleic Acids Res. 26 (6), 1369–1372.

ten Dam, E.B., Pleij, C.W., Bosch, L., 1990. RNA pseudoknots: translational frameshifting and readthrough on viral RNAs. Virus Genes 4 (2), 121–136.

Thiel, V., Ivanov, K.A., Putics, A., Hertzig, T., Schelle, B., Bayer, S., Weissbrich, B., Snijder, E.J., Rabenau, H., Doerr, H.W., Gorbalenya, A.E., Ziebuhr, J., 2003. Mechanisms and enzymes involved in SARS coronavirus genome expression. J. Gen. Virol. 84 (Pt. 9), 2305–2315.

Thompson, J.D., Higgins, D.G., Gibson, T.J., 1994. CLUSTAL W: improving the sensitivity of progressive multiple sequence alignment through sequence weighting, position-specific gap penalties and weight matrix choice. Nucleic Acids Res. 22 (22), 4673–4680.

Yusupova, G.Z., Yusupov, M.M., Cate, J.H., Noller, H.F., 2001. The path of messenger RNA through the ribosome. Cell 106 (2), 233–241.

Zuker, M., 2003. Mfold web server for nucleic acid folding and hybridization prediction. Nucleic Acids Res. 31 (13), 3406–3415.